Journal of Applied Polymer Science

Synthesis and Characterization of Polypyrrole-Au Coated SiO_2@Poly(4-vinylpyridine) Composites

Linchao Lu, Wenqin Wang, Wujin Cai, Zhong-Ren Chen
Faculty of Materials Science and Chemical Engineering, Ningbo University, Ningbo 315211, People's Republic of China
Correspondence to: W. Wang (E-mail: wqwang@126.com) or Z.-R. Chen (E-mail: chenzhongren@nbu.edu.cn)

ABSTRACT: Microspheres with silica as core and poly(4-vinylpyridine) (P4VP) as shell were synthesized. $AuCl_4^-$ ions were bound by P4VP chains to form the complex, which acted both as an oxidant of pyrrole monomers and as a source of Au atoms. By vapor phase polymerization, the PPy and Au nanoparticles were simultaneously formed on the surfaces of SiO_2@P4VP microspheres. The core-shell structure was confirmed by transmission electron microscopy. The surface morphologies of the composites were observed by scanning electron microscopy. The molecular structures of composites were characterized in detail by Raman spectra, X-ray diffraction, and X-ray photoelectron spectroscopy. © 2012 Wiley Periodicals, Inc. J. Appl. Polym. Sci. 128: 4130–4135, 2013

KEYWORDS: poly(4-vinylpyridine); microsphere; Au nanoparticle; polypyrrole

Received 18 July 2012; accepted 24 September 2012; published online 17 October 2012
DOI: 10.1002/app.38636

INTRODUCTION

There has been increasing interest on the preparation of conducting polymer and conducting polymer matrix composite due to their potential applications in solar cells,[1,2] catalysis,[3,4] surface enhance Raman scattering (SERS),[5–7] and so forth. Among various conducting polymer matrix composites, conducting polymer-noble metal (gold, silver, and palladium)/composite has attracted considerable attention because it combines excellent environmental stability, good redox properties of conducting polymers[8,9] and the unique optical, catalytic, and electrochemical properties of noble metal nanoparticles.[10–12] So far, a number of strategies for the synthesis of conducting polymer-the noble metal composites have been reported.[13–17] For example, Shi and coworkers[13] prepared the flower-like Pd nanoparticles on polypyrrole (PPy) film by electrochemical deposition. The as-prepared PPy-Pd composite exhibited high SERS-activity and the enhancement factor was measured to be as high as 10^5 for 4-mercaptopyridine. Feng et al.[14] fabricated the polyaniline-Au composite via electrostatic assembly, and the composite showed high catalytic activity for the oxidation of dopamine.

Using the template method to prepare the conducting polymer-metal composites has also been reported.[15–17]

Recently, one-step synthesis of conducting polymer-noble metal composite using metal salts ($AgNO_3$,[18–20] $Pd(C_2H_3O_2)_2$,[21] and $PdCl_2$[4,22]) as an oxidant has developed. This method bases on oxidation of pyrrole monomer and the reduction of the metal salts, yielding PPy and elemental metal simultaneously. For example, Fujii et al. used $PdCl_2$ as the oxidant to oxidize pyrrole monomer, and the formation of PPy and reduction reaction of Pd^{2+} ions to Pd atoms occurred simultaneously. As-obtained PPy-Pd composite can be used as an efficient catalyst for Suzuki-type coupling reaction.[4]

Tetrachloroauric acid ($HAuCl_4$) as an oxidant in the presence of polystyrene-*b*-poly(2-vinylpyridine) copolymer micelles for fabrication of PPy-Au nanocomposite has been reported.[23] In this method, the $AuCl_4^-$ ions attached to poly(2-vinylpyridine) chain acted both as oxidant and as a source of Au atoms. However, its disadvantage involved high-cost block polymer and complicated self-assembly process in toluene. Herein, we describe a novel approach to prepare PPy-Au on the surface of SiO_2@Poly(4-vinylpyridine) (P4VP) microsphere. The SiO_2@P4VP microspheres are treated with $HAuCl_4$, and $AuCl_4^-$ ions are bound by P4VP chains to form SiO_2@P4VP-$HAuCl_4$ complex by electrostatic adsorption due to positively charged NH groups of pyridine.[23,24] The complex can act as an oxidant for pyrrole monomer. By vapor phase polymerization, the PPy and Au nanoparticles (Au NPs) are formed simultaneously on the surfaces of SiO_2@P4VP microspheres. Because the chain of poly(4-vinylpyridine) can attach various metal salts, the strategy is simple and versatile for synthesis of other conducting polymer-metal composite.

EXPERIMENTAL

Materials and Methods

Materials. Tetraethylorthosilicate (TEOS), divinylbenzene (DVB), and 4-vinylpyrinde (4-VPy) were purchased from Aldrich.

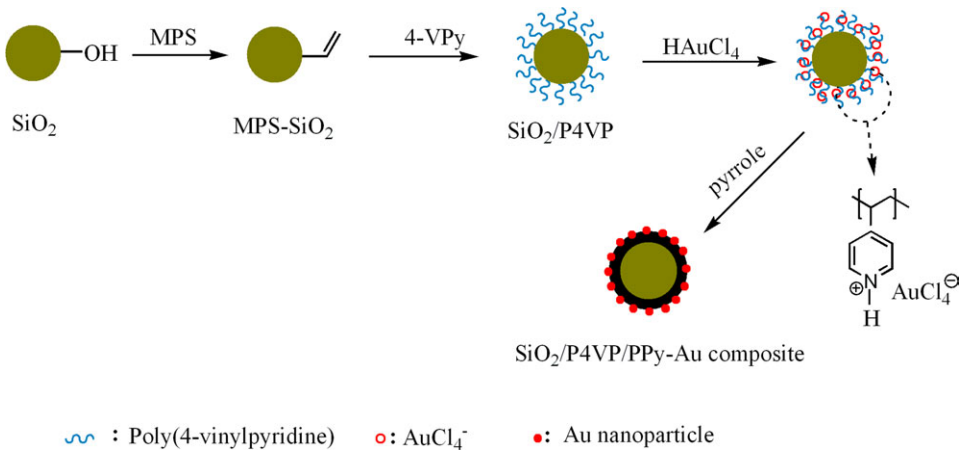

Scheme 1. The fabrication of the SiO_2@P4VP@PPy-Au composite. [Color figure can be viewed in the online issue, which is available at wileyonlinelibrary.com.]

3-(Trimethoxysilyl) propyl methacrylate (MPS) was purchased from Alfa. 2,2′-azobis (isobutyronitrile) (AIBN), acetonitrile, pyrrole, and chloroauric acid trihydrate ($HAuCl_4 \cdot 3H_2O$) were obtained from Sinopharm Chemical Reagent Co. (Shanghai, China). DVB was washed with 5% aqueous sodium hydroxide and water, then dried over anhydrous magnesium sulfate before use. 4-VPy, MPS, and pyrrole were distilled under reduced pressure before use. AIBN was recrystallized from methanol. Acetonitrile was dried over calcium hydride and purified by distillation. Other reagents were of analytical grade and used as received without further treatment.

Preparation of SiO_2@P4VP@PPy-Au Composites. The MPS-modified silica and SiO_2@P4VP microsphere were prepared according to Ref. 25. A total of 0.1 g SiO_2@P4VP microspheres were dispersed into 10 mL of 10 m*M* $HAuCl_4$ aqueous solution, and the mixed solution was stirred for 12 h. The excessive $HAuCl_4$ was removed by centrifugalization, and the obtained SiO_2@P4VP-$HAuCl_4$ complex was redispersed in 10 mL of deionized water via ultrasound to form colloidal solution. A certain amount of above colloidal solution was dropped on the silica substrate and dried by N_2 flow. Subsequently, the silica substrate was placed into a closed container filled with saturated pyrrole vapor, and the vapor phase polymerization was allowed for 24 h at room temperature. The obtained product was dried in vacuum oven at 60°C for 24 h.

Characterization

Scanning electron microscopy (SEM, S-4800) and transmission electron microscope (TEM, H-7650) were used to observe the morphologies of the composites. X-ray diffraction (XRD, RigakuD/max-1200), Raman spectra (HR800), and X-ray photoelectron spectroscope (XPS, Axis Utltra DLD) were used to characterize the composite. Thermogravimetric (TG) analysis was determined with a Perkin–Elmer thermogravimetric analyzer (TG-DTA, SSC-5200) at a heating rate of 10°C min^{-1} in N_2 from room temperature up to 900°C.

RESULTS AND DISCUSSION

The preparation of the SiO_2@P4VP@PPy-Au composites is described in Scheme 1. First, 4-VPy monomers are polymerized on the surface of the MPS-modified SiO_2 to form SiO_2@P4VP microspheres. Second, the SiO_2@P4VP microspheres are immersed in $HAuCl_4$ aqueous solution and $AuCl_4^-$ ions are adsorbed to the P4VP chains. Finally, SiO_2@P4VP@PPy-Au composite is obtained by the vapor phase polymerization.

Morphology

Figure 1(a), shows the low-resolution SEM image of SiO_2@P4VP microspheres. Figure 1(b) is a higher magnification SEM image obtained from a selected area of Figure 1(a) and clearly shows that SiO_2@P4VP microsphere with about 450 nm in diameter has relatively smooth surface. The core-shell structure of the microsphere is confirmed by their TEM images [as shown in Figure 1(c)]. The sharp dark-light contrast indicates that the particles have P4VP shells (light contrast) and SiO_2 cores (dark contrast).

After vapor phase polymerization, the SEM images of the obtained SiO_2@P4VP@PPy-Au composite is shown in Figure 2(a,b). The outside nanoparticles in Figure 2(b) and the corresponding dark spots in Figure 2(c) are Au NPs. From these images, it is found that the distribution of Au NPs on the surfaces of the products is very nonuniform, as a set of agglomerated clusters. Usually, the nanoparticles trend aggregation to reduce the surface energy. The Au NPs are charged, and the resulting electrostatic repulsion can prevent or lower the aggregation.[26] In our experiment, formed Au NPs without any electric charge on the surface are small in diameter. So, the aggregation is unavoidable. In addition, the relatively low coverage of Au NPs is observed. The possible explanation is that the P4VP shell is not enough thick in our experiment, which leads to the amount of the $AuCl_4^-$ ions absorbed on the P4VP shell is insufficient. It may be effective to improve Au NPs coverage if more 4-vinylpyrinde monomers are polymerized to increase the thickness of P4VP shell.

Structural Characterization

Figure 3 shows the Raman spectra of SiO_2, SiO2@P4VP microspheres, and SiO_2@P4VP@PPy-Au composites. As shown in Figure 3(b), the spectrum of SiO_2@P4VP microspheres has three strong bands centered at 996, 2922, and 3052 cm^{-1}, which are assigned to ring breathing, aliphatic CH_2 asymmetric stretching, and CH asymmetric ring stretching in the P4VP, respectively.[27] However, these peaks are absent in the spectrum

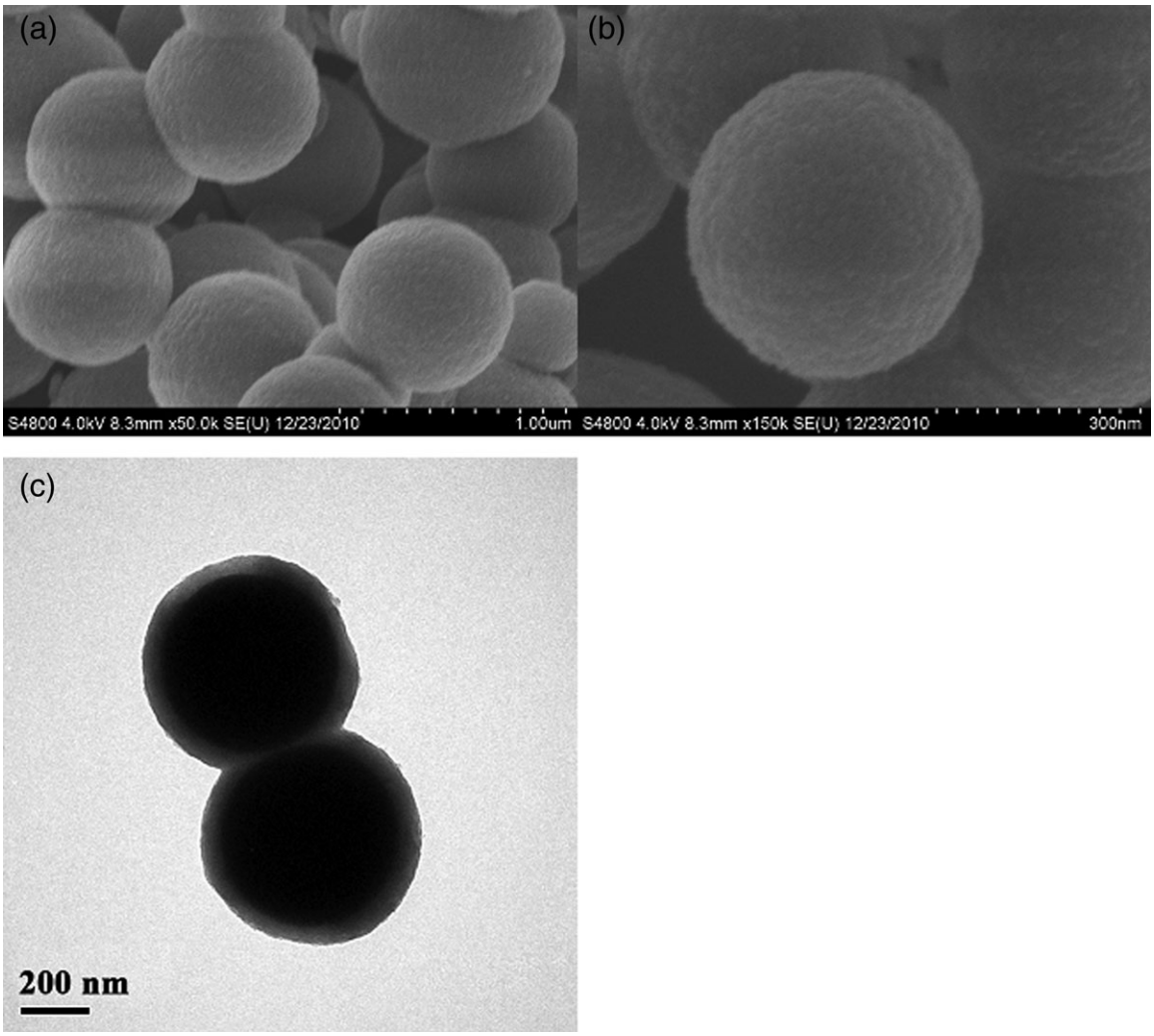

Figure 1. SEM images of SiO_2@P4VP microspheres: (a) low resolution; (b) higher resolution; (c) TEM image of SiO_2@P4VP microspheres.

of the SiO_2@P4VP@PPy-Au composites [Figure 3(c)]. Figure 3(c) exhibits a strong peak attributed C—C stretching of PPy backbone at ca., 1590 cm^{-1}. The double peaks at ca., 1051 and 1082 cm^{-1} are assigned to be the C—H in-plane deformation. The other double peaks at 1335 and 1381 cm^{-1} are attributed to be the ring stretching mode of PPy. The bands at 941 and 980 cm^{-1} are assigned to the ring deformation associated with dication (dipolarion) and radical cation (polaron) of PPy, respectively. The results are good agreement with the reported data,[28–31] which prove that PPy is formed.

XRD spectrum of the SiO_2@P4VP@PPy-Au composites is shown in Figure 4. Four strong bands with maximum intensity at 38.2°, 44.2°, 64.6°, and 77.6° are observed, which represents Bragg's reflections from (111), (200), (220), and (311) planes of Au.[32] For the above data, Au can be further confirmed to exist on the surface of the composite. In addition, the size of Au crystallite using Scherrer Formula is estimated to be about 30 nm, which was in general accord with that of Au in TEM image in Figure 2.

The molecular structure of the composites was further characterized by XPS. Survey spectrum of SiO_2@P4VP@PPy-Au composite is depicted in Figure 5(a). The main peaks, C 1s, O 1s, and N 1s are observed at 285, 400, and 532eV, respectively. The signal due to Cl 2p indicates that the cationic PPy chains are doped with chloride anions (from $AuCl_4^-$ ions). The Au 4f signal is detected, and the doublet with BE at 83.6 eV (Au $2f_{7/2}$) and 87.2 eV (Au $2f_{5/2}$), as shown in Figure 5(b), can be assigned to the gold nanoparticles.[33] In addition, a small component at ca., 86–87 eV is assigned to the presence of Au(III). These species are possibly due to incomplete reduction of $[AuCl_4]^-$ during gold nanoparticles synthesis.[34]

The peak-fitted N1s core-line spectrum of SiO_2@P4VP@PPy-Au composite [Figure 5(c)] shows that three nitrogen environments are present. The peak at 398.6 and 399.8 eV are attributed to the uncharged deprotonated imine (=N—) nitrogen species and neutral nitrogen atoms (—NH—) in PPy. The two peaks (at 400.8 and 402.2 eV) are assigned to positively charged nitrogen (N^+) species in PPy.[35] The doping level of PPy is calculated from the ratio of the peak area of N^+ to the total of N 1s.[36] The results show that the doping level of PPy in the composite is 0.328, which is higher than that of neat PPy (0.263). The existence of protonated amine is supposed to lead to the attachment of the gold nanoparticles to the SiO_2@P4VP@PPy particles surface.

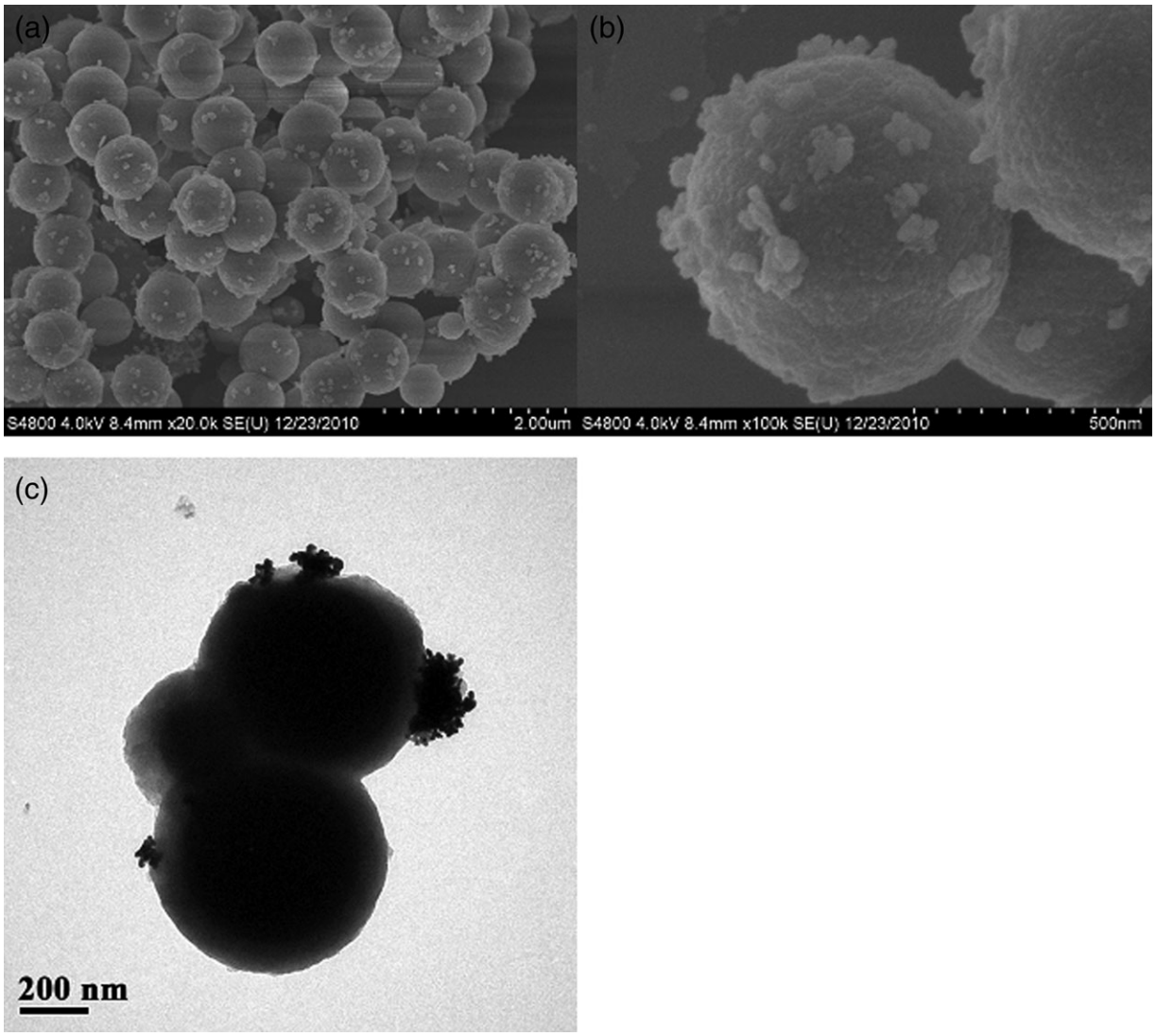

Figure 2. SEM images of SiO_2@P4VP/PPy-Au composites: (a) low resolution; (b) higher resolution; (c) TEM image of SiO_2@P4VP@PPy-Au composites.

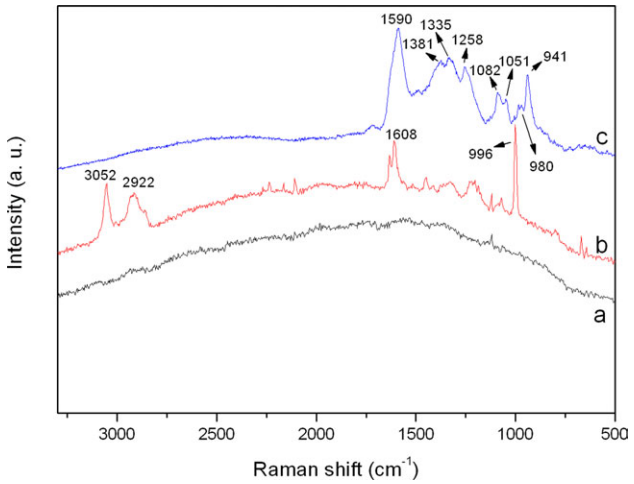

Figure 3. The Raman spectra of SiO_2 (a), SiO_2@P4VP microparticles (b), and SiO_2@P4VP@PPy-Au composites (c). [Color figure can be viewed in the online issue, which is available at wileyonlinelibrary.com.]

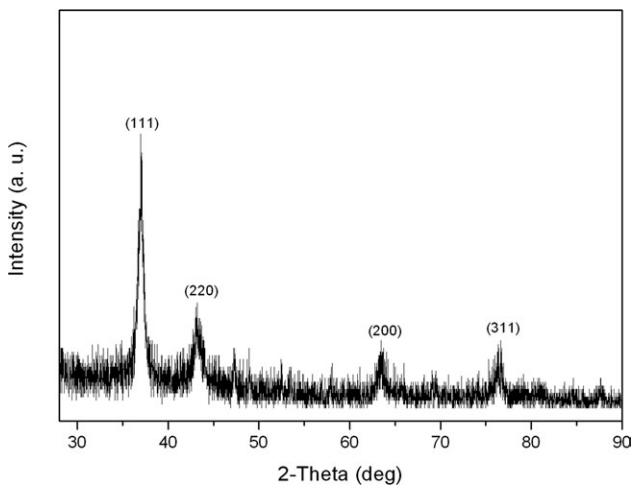

Figure 4. XRD pattern of the SiO_2@P4VP@PPy-Au composites.

Applied Polymer SCIENCE

TG Analysis

The TG curve of SiO_2@P4VP microspheres is showed in Figure 6(a). The initial weight loss below 200°C is due to the evaporation of moisture. The significant loss of the weight takes place in the 380°C–450°C interval. The percentages of residual

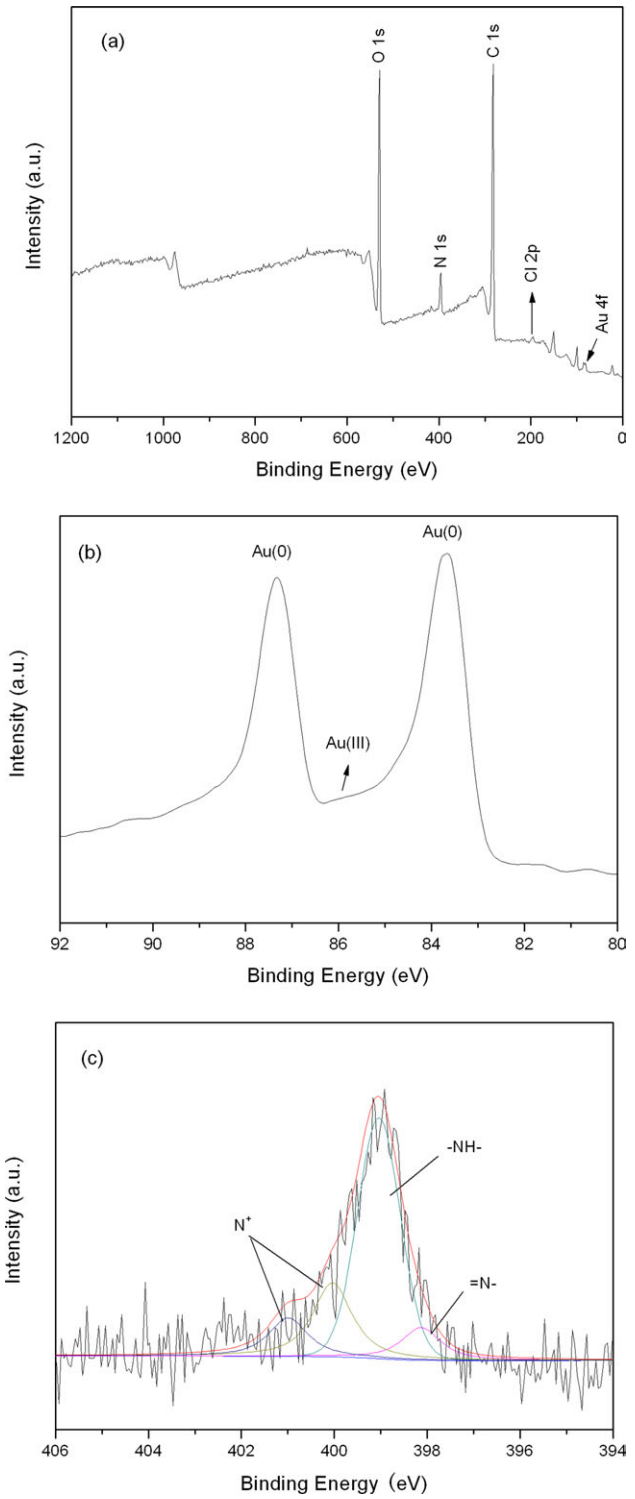

Figure 5. XPS spectra survey spectra (a), high-resolution Au 4f spectrum (b), and high-resolution N(1s) spectra (c). [Color figure can be viewed in the online issue, which is available at wileyonlinelibrary.com.]

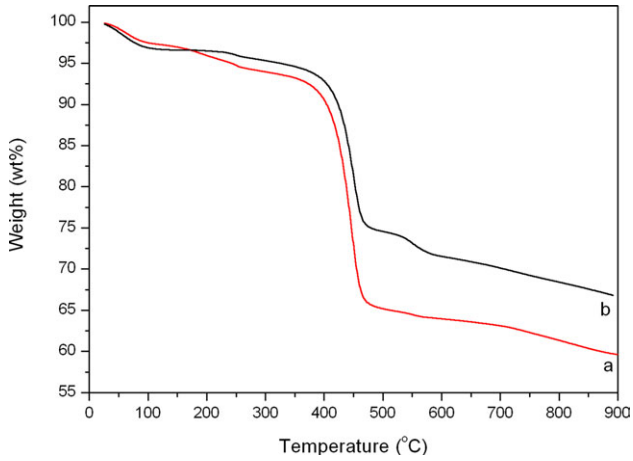

Figure 6. TG curves of SiO_2@P4VP microsphere (a) and SiO_2@P4VP@PPy-Au composites (b). [Color figure can be viewed in the online issue, which is available at wileyonlinelibrary.com.]

SiO_2 and a carbonized layer from the polymer is about 60 wt %. The curve of the SiO_2@P4VP@PPy-Au microspheres is presented in Figure 6(b) and is similar to that of the SiO_2@P4VP microspheres. Comparing curve a with curve b, the ratio of the mass of the Au-PPy deposite to the substrate balls is estimated crudely to be about 7 wt %. The continuous weight loss between 450°C and 900°C interval is mainly caused by the decomposition of the PPy to form various N-containing byproducts such as HCN and N_2, thus leading to produce poly-condensed graphitic species.[37–39]

CONCLUSIONS

In summary, we have successfully synthesized SiO_2@P4VP@PPy-Au composite by vapor phase polymerization under ambient condition. The composites were characterized in terms of size, morphology, and core-shell structure. Because the P4VP chains can absorb various kinds of metal salts, the approach may open up new opportunities to fabricate the other metal/conducting polymers composites with potential in various applications.

ACKNOWLEDGMENTS

This work was sponsored by K. C. Wong Magna Fund in Ningbo University, Research Foundation for Advanced Talents of Ningbo University (RCL2008003), and Student Research and Innovation Program of Zhejiang Province (2011R405052).

REFERENCES

1. Hao, Y. Z.; Yang, M. Z.; Li, W. H.; Qiao, X. B.; Zhang, L.; Cai, S. M. *Solar Energy Mater. Sol. Cells* **2000**, *60*, 349.
2. Zhou, N. J.; Guo, X. G.; Ortiz, R. P.; Li, S. Q.; Zhang, S. M.; Chang, R. P. H.; Facchetti, A.; Marks, T. J. *Adv. Mater.* **2012**, *24*, 2242.
3. Yao, T. J.; Wang, C. X.; Wu, J.; Lin, Q.; Lv, H.; Zhang, K.; Yu, K.; Yang, B. J. *Colloid Interface Sci.* **2009**, *338*, 573.
4. Fujii, S.; Matsuzawa, S.; Nakamura, Y.; Ohtaka, A.; Teratani, T.; Akamatsu, K.; Tsuruoka, T.; Nawafune, H. *Langmuir* **2010**, *26*, 6230.

5. Wang, W. Q.; Li, W. L.; Zhang, R. F. *Mater. Chem. Phys.* **2010**, *124*, 385.
6. Wang, W. Q.; Zhang, R. F. *Synth. Met.* **2009**, *159*, 1332.
7. He, Y. H.; Yuan, J. Y.; Shi, G. Q. *J. Mater. Chem.* **2005**, *15*, 859.
8. Roucoux, A.; Schulz, J.; Patin, H. *Chem. Rev.* **2002**, *102*, 3757.
9. Menon, V. P.; Martin, C. R. *Anal. Chem.* **1995**, *67*, 1920.
10. Peng, X. H.; Pan, Q. M.; Rempel, G. L. *Chem. Soc. Rev.* **2008**, *37*, 1619.
11. Eryazici, I.; Moorefield, C. N.; Newkome, G. R. *Chem. Rev.* **2008**, 108, 1834.
12. Crooks, R. M.; Zhao, M. Q.; Sun, L.; Chechik, V.; Yeung, L. K. *Acc. Chem. Res.* **2001**, *34*, 181.
13. Li, Y.; Lu, G. W.; Wu, X. F.; Shi, G. Q. *J. Phys. Chem. B* **2006**, *110*, 24585.
14. Feng, X. M.; Mao, C. J.; Yang, G.; Hou, W. H.; Zhu, J. J. *Langmuir* **2006**, *22*, 4384.
15. Shin, H. J.; Hwang, I.-W.; Hwang, Y.-N.; Kim, D.; Han, S. H.; Lee, J.-S.; Cho, G. *J. Phys. Chem. B* **2003**, *107*, 4699.
16. Xing, S. X.; Tan, L. H.; Yang, M. X.; Pan, M.; Lv, Y. B.; Tang, Q. H.; Yang, Y. H.; Chen, H. Y. *J. Mater. Chem.* **2009**, *19*, 3286.
17. Wang, W. Q.; Li, W. L.; Zhang, R. F.; Wang, J. *J. Synth. Met.* **2010**, *160*, 2255.
18. Chen, A.; Kamata, K.; Nakagawa, M.; Iyoda, T.; Wang, H.; Li, X. *J. Phys. Chem. B* **2005**, *109*, 18283.
19. Chen, A.; Wang, H.; Li, X. *Chem. Commun.* **2005**, 14, 1863.
20. Fujii, S.; Aichi, A.; Akamatsu, K.; Nawafune, H.; Nakamura, Y. *J. Mater. Chem.* **2007**, *17*, 3777.
21. Vasilyeva, S. V.; Vorotyntsev, M. A.; Bezverkhyy, I.; Lesniewska, E.; Heintz, O.; Chassagnon, R. *J. Phys. Chem. C* **2008**, *112*, 19878.
22. Lu, L. C.; Wang, W. Q.; Cai, W. J.; Chen, Z. R. *J. Polym. Mater.* **2012**, *29*, 253.
23. Selvan, S. T.; Spatz, J. P.; Klok, H.-A.; Möeller, M. *Adv. Mater.* **1998**, *10*, 132.
24. Zinovyeva, V. A.; Vorotyntsev, M. A.; Bezverkhyy, I.; Chaumont, D.; Hierso, J.-C. *Adv. Funct. Mater.* **2011**, *21*, 1064.
25. Liu, G. Y.; Li, L. Y.; Yang, X. L.; Dai, Z. *Polym. Adv. Technol.* **2008**, *19*, 1922.
26. Westcott, S. L.; Oldenburg, S. J.; Lee, T. R.; Halas, N. *J. Langmuir* **1998**, *14*, 5396.
27. Gailliez-Degremont, E.; Bacquet, M.; Laureyns, J.; Morcellet, M. *J. Appl. Polym. Sci.* **1997**, *65*, 871.
28. Liu, Y.; Hwang, B.; Jian, W.; Santhanam, R. *Thin Solid Films* **2000**, *374*, 85.
29. Liu, Y.; Hwang, B. *Synth. Met.* **2000**, *113*, 203.
30. Gongcalves, A. B.; Mangrich, A. S.; Zarbin, A. J. G. *Synth. Met.* **2000**, *114*, 119.
31. Chen, F. E.; Shi, G. Q.; Fu, M. X.; Qu, L. T.; Hong, X. Y. *Synth. Met.* **2003**, *132*, 125.
32. Huang, K.; Zhang, Y. J.; Han, D. X.; Shen, Y. F.; Wang, Z. J.; Yuan, J. H.; Zhang, Q. X.; Niu, L. *Nanotechnology* **2006**, *17*, 283.
33. Rabbania, M. M.; Kob, C. H.; Baec, J. S.; Yeumd, J. H.; Kima, I. S.; Oh, W. *Colloid. Surf. A* **2009**, *336*, 183.
34. Mangeney, C.; Bousalem, S.; Connan, C.; Vaulay, M.-J.; Bernard, S.; Chehimi, M. M. *Langmuir* **2006**, *22*, 10163.
35. Neoh, K. G.; Lau, K. K. S.; Wong, V. V. T.; Kang, E. T.; Tan, K. L. *Chem. Mater.* **1996**, *8*, 167.
36. Liu, Y. C.; Hwang, B. J. *Thin Solid Film.* **2000**, *360*, 1.
37. Han, C.; Lee, J.; Yang, R.; Han, C. *Chem. Mater.* **2001**, *13*, 2656.
38. Jang, J.; Oh, J. H. *Adv. Funct. Mater.* **2005**, *15*, 494.
39. Dong, H.; Jones, W. E., Jr. *Langmuir* **2006**, *22*, 11384.